

PROCEEDINGS OF THE SECOND INTERNATIONAL SYMPOSIUM ON

QUANTUM CONFINEMENT PHYSICS AND APPLICATIONS

Editors

M. Cahay
University of Cincinnati
Cincinnati, Ohio

S. Bandyopadhyay
University of Notre Dame
Notre Dame, Indiana

J.P. Leburton
University of Illinois
Urbana, Illinois

A.W. Kleinsasser
T.J. Watson Research Center
Yorktown Heights, New York

M.A. Osman
Washington State University
Pullman, Washington

DIELECTRIC SCIENCE AND TECHNOLOGY, ELECTRONICS
AND LUMINESCENCE AND DISPLAY MATERIALS DIVISIONS

Proceedings Volume 94-17



THE ELECTROCHEMICAL SOCIETY, INC.,
10 South Main St., Pennington, NJ 08534-2896

ELECTRON-WAVEGUIDE Y BRANCHES AS CURRENT SWITCHES

Nadir Dagli, Mason Thomas, Muralidhar Rao, Mani Sundaram, and Arthur Gossard
Electrical and Computer Engineering Department
University of California
Santa Barbara, CA 93106

ABSTRACT

In this work an electron waveguide Y branch is experimentally studied. The aim of the study is to observe current switching based on phase coherent interactions of electrons in the Y branch. It is found that current switching indeed occurs but due to a different mechanism. Experimental results indicate that phase coherence of the electrons is not maintained over the entire Y branch. Electrons stay phase coherent only over short sections of the output branches creating quantized conductance. As a result Y branch behaves as a junction of two independent quantized conductances. It is possible to observe current switching in such a junction if the quantized conductances of the output branches are not synchronized. This mode of operation is expected to be more robust than the switching based on modal evolution and can result in novel electronic devices with gain.

INTRODUCTION

Recent advances in material growth and lithography have made it possible to fabricate electronic structures with dimensions smaller than the phase coherence length of electrons. In such structures electrons propagate without making any phase randomizing collisions, hence the phases of the electron waves entering and leaving the structure are deterministically related. If such transport is combined with quantum confinement the so called electron waveguides can result. In practice electron waveguides are realized as short quantum wires connecting two two dimensional electron gas reservoirs. The conductance of an electron waveguide is quantized if the two dimensional quantum confinement results in subband spacings larger than the energy spread of the electrons contributing to net current flow through it and the transport is phase coherent [1], [2]. Each one dimensional subband in such a waveguide contributes a conductance of $2e^2/h$ multiplied by a transmission probability [3]. This creates a situation analogous to electromagnetic waveguiding. This analogy prompted a great deal of interest in the electrical engineering community since using electron waveguides new and novel devices operating like photonic guided-wave devices can be created. Several such proposals have already been made and analyzed theoretically [4], [5], [6], [7], [8]. However, one has to be careful in utilizing this analogy, because there are differences in addition to similarities between electromagnetic and electronic waveguiding. In both cases phase coherent transmission and guided modes or subbands are possible. But in electronic waveguiding the phase coherence length tends to be at the order of a few de Broglie wavelengths of the electrons contributing to the transport. This is much shorter than the phase coherence length in electromagnetic waveguiding, which could be millions of wavelengths. Furthermore, at

any finite temperature or bias the electrons injected into an electron waveguide have a certain energy spread. Therefore they are not monoenergetic, equivalently they are not monochromatic. In other words one does not have the equivalent of lasers or microwave oscillators for electronic waveguiding. Moreover, photons are bosons and there is no fundamental limit on the number of photons in a particular mode other than practical considerations such as material breakdown or nonlinearities. On the other hand, electrons are fermions and obey Pauli exclusion principle. As a result, the current carrying capacity of an electron waveguide mode is limited to 88 nanoAmperes per millivolt applied across it. This overall assessment has important implications. Any structure that relies on the phase coherent interactions of electrons should be only a few electron wavelengths long. Furthermore, it should operate over a wide electron energy or wavelength range. In other words it should be broadband. Moreover, the limitations on the current that a mode can support could have significant effects in realizing structures with gain. Obviously a structure which can operate with multimoded waveguides can carry more current, hence is desirable. These implications create difficulties for interference devices such as electron wave directional couplers [7], [8]. On the other hand, there are optical devices that address some of these difficulties and may provide a parallel for practical electronic devices based on electron waveguiding. In this work one such device, which is the analog of the Y branch in integrated optics also known as the digital switch was experimentally studied [9], [10]. In the next section the basic principle of operation of the Y branch as a digital switch is briefly described. Next, experimental results on an electron waveguide Y branch are given. It is demonstrated that the observed switching behavior originates due to a mode of operation different than modal evolution in a Y branch. Next, it is shown this mode of operation is more robust than the expected modal evolution and could lead to active devices operating at realistic temperatures and bias conditions. Finally, conclusions are given.

Y BRANCH AS A DIGITAL SWITCH

This device is a Y branch of single mode waveguides which is schematically illustrated in Figure 1. An incoming wave will split equally between the output branches with very little back reflection provided that the device is symmetrical, i.e., the output branches are identical, and the apex angle Q of the Y branch is small so that the branching is adiabatic. On the other hand, if an asymmetry is created between the output branches the input wave is monotonically coupled to the output branch with the higher index in the case of optical waves or lower potential energy in the case of electron waves, as indicated schematically in Figure 1. For optical waves this coupling occurs over wide wavelength ranges and for both polarizations [9], [10]. Furthermore, it has digital characteristics. In other words, whatever couples to one branch does not couple back to the other branch if the asymmetry between the branches is further increased. Therefore, there is no need to create a precise asymmetry between the branches. This is because the switching is achieved without the need for modal interference. The incoming wave propagates as the local eigenmode of the branching waveguides and evolves into the mode of one of the output waveguides. The same device was also theoretically studied for electron waves [11]. It is shown that even in the case of multimoded waveguides and branching angles of 60° , it is possible to switch electrons to the arm with the lower potential energy over a fairly large energy spread of incoming electrons. The structure formed this way can switch an incoming wave to either one of the arms of the Y branch if the properties of the output branches are modulated by the external voltages. The fact that the switching has digital characteristics, can occur in the presence of multimoded waveguides, and for a fairly large

energy spread of the incoming electrons makes this device very attractive due to the reasons outlined in the introduction.

EXPERIMENTAL RESULTS AND DISCUSSION

The devices used in the experiments are fabricated using the split gate scheme as illustrated in figure 2. The starting material is a high quality modulation doped conventional two dimensional electron gas (2DEG) sample. In this structure electrons are quantum confined at the planar interface of a GaAs/Al_{0.3}Ga_{0.7}As heterojunction some distance d below the surface. Schottky gates and ohmic contacts are fabricated at the surface of the sample as shown in figure 2. When the Schottky gates are sufficiently negatively biased, electrons underneath the gates are repelled or depleted. This creates a narrow channel of electrons in the form of a Y branch. If the width and the strength of the confining electrostatic potential in these channels are appropriate for two dimensional quantum confinement and the transport of the electrons is phase coherent, they will function as electron waveguides. Changing the voltage on the Schottky gates changes the width and the strength of the electrostatic potential. Therefore the waveguiding geometry can be tuned by external voltages and an asymmetry between the output branches can be created. As described earlier, due to this asymmetry the input electron wave is expected to couple to the output branch with the lower potential. Externally, this is observed as switching of the incoming current to one of the output branches as a function of the voltages applied to the gates. In the experiments, two devices with different dimensions and material designs were used. These devices will be designated as A and B. For A the 2DEG was 1200Å deep and the mobility and the carrier concentration at 4.2 K were $1.1 \times 10^6 \text{cm}^2/\text{V}\cdot\text{sec}$ and $3.0 \times 10^{11} \text{cm}^{-2}$ respectively. For B the 2DEG was 500Å deep. The mobility and the carrier concentration of the 2DEG at 4.2 K were $4.2 \times 10^5 \text{cm}^2/\text{V}\cdot\text{sec}$ and $4.8 \times 10^{11} \text{cm}^{-2}$ respectively. For both devices, $a = 800 \text{Å}$ and the apex angle of the Y branch is 35° . The other dimension b was 5000 Å and 3000Å for A and B respectively.

Figure 3 shows a schematic describing the measurement conditions. A current or voltage source is applied to the input of the Y. One of the gate voltages, V_{g3} , is kept constant, while the voltages applied to the side gates, V_{g1} and V_{g2} , are changed and the currents from the branches of the Y were recorded. Figure 4(b) shows the currents in the output branches for device A as a function of the gate voltages V_{g1} and V_{g2} when at the input a constant current is sourced. The output currents are mirror images of one another since their sum is constant. The timing of the gate voltages with respect to one another is also shown in figure 4(a). Both V_{g1} and V_{g2} were ramped from 0 to -1.8 V and then back to 0V. V_{g2} was kept to be zero until V_{g1} reached -0.4 volts. In this experiment the intention was to create enough asymmetry between the two output branches to observe monotonic switching of the current to the wider branch with the lower potential. In this case there are two different bias conditions. In the areas outside the markers, i.e., when V_{g2} is larger than -1.4V, both gate voltages decrease or increase at the same time with a -0.4 V offset between them. Under this bias condition oscillations are observed in both currents. On the other hand in between the markers gate voltages change in opposite directions, i.e., as one of them increases the other one decreases. Under this bias condition both currents change monotonically. Specifically I_1 increases and I_2 decreases as expected since branch 1 is getting wider and branch 2 is getting narrower. The results of the same measurement on the same device at 0.3K are shown in figure 4(c). The same general

features are again observed. The oscillations are stronger when gates are driven in the same direction. When gates are driven in opposite directions, i.e., in push pull fashion, currents still change monotonically but features start to appear. Since the behavior of both currents under two different bias conditions are quite different they are investigated further. In one case the offset between V_{g1} and V_{g2} was increased to $-1.74V$ as shown in figure 5. For device A the 2DEG region under the gates does not deplete until the gate voltage reaches $-0.4V$. Therefore in the areas outside the markers there is only one output branch. For example, when V_{g1} decreases from 0 to $-1.8V$ the only output branch is branch one. As V_{g1} decreases this branch gets narrower and current through it decreases with a resulting increase in I_2 . However, in between the markers the gates are driven in opposite directions. Then the output currents change monotonically as before over the entire range. In this case I_1 increases and I_2 decreases as expected since branch 1 is getting wider and branch 2 narrower. This result seems to be consistent with expected digital switch operation. On the other hand if there is not any offset between the side gates, i.e., if the same voltage is applied to them oscillations of both currents are observed over the entire bias range. Figures 6(a) and (b) show the result of such an experiment on device B. In this case the same bias voltage is applied to both side gates and in figure 6(a) the input is driven by a constant current source. The output currents oscillate and even cross over. Although the external voltages forming the channels are the same, there is a built in asymmetry between the channels. This simply results from unavoidable fabrication difficulties which makes the fabrication of two identical gate patterns of very small size very difficult. As a result one of the channels is wider than the other, hence will always have a lower potential. Yet the current does not switch over monotonically to the arm with the lowest potential as expected from a coherent wave picture. This behavior is contrary to what is expected based on digital switch operation.

To understand these seemingly conflicting results the conductances of the both channels were measured. Figure 7 shows the individual channel conductances of device A corresponding to the measurement shown in Figure 4(b). On each curve markers indicate when the gate voltage changes from down sweep to an up sweep. It is seen that the individual channel conductances for the down and up sweeps of the gate voltages are identical. In other words these two curves have mirror symmetry with respect to the perpendicular lines passing through the markers. If this symmetry is utilized and the conductances measured when the gates are up and down swept are folded into a single curve, it is immediately observed that they behave very much like the conductance of an individual channel. There is a certain offset between them due to the biasing scheme. When the gates are driven in the same direction they follow one another and even cross over. This results in oscillations in the channel currents. When the gates are driven in push pull one channel conductance increases and the other decreases, which results in a monotonic current change. This discussion suggest that the output branches of the Y behave as independent channels and the wavefunction coherence is not preserved over the entire Y branch.

This is more obvious for device B. In this case, quantum confinement is stronger since 2DEG is shallower. Figure 6(b) shows the results of the measurement on device B with a constant voltage is applied across the Y rather than a constant current into the Y as done earlier. In this case, current flowing through the arms of the Y shows quantized steps. This is the signature of electron waveguiding in a single electron waveguide. The quantized steps indicate the number of modes propagating in each arm. Each mode contributes a conductance $2e^2/h$ multiplied by a transmission coefficient to the conductance

of the arm. This again shows that the branches of the Y behave as uncoupled individual waveguides. However, the conductances of the output branches are not synchronous with one another. In other words, the number of modes in each arm or the transmission through each arm changes asynchronously. This is due to the asymmetry built into the device resulting in one of the arms always having a lower potential compared to the other. Yet the current does not switch over monotonically to the arm with the lowest potential as expected from a coherent wave picture. But the current in each arm oscillates as the number of allowed modes changes, changing the transmission through each arm. This is verified by comparing the constant current and constant voltage measurements shown in figure 6(a) and (b). At the crossover points of the constant voltage measurement both arms have the same number of modes or the same conductance, and as a result currents also cross over in the constant current measurement. Likewise, minima and maxima of the constant current measurement occur at the points of largest difference between the conductances of both arms. Therefore, oscillations arise from the difference in the number of modes of each arm, rather than coherent electron wave interaction over the entire Y branch. From a wave point of view, this situation is analogous to a junction of two short rectangular metallic waveguides excited by radiation with a very short phase coherence length. If the radiation stays coherent over the short waveguide sections, the transmission through each arm can be modulated changing the number of modes it supports by moving the walls of the waveguide in and out. Therefore, the energy coming out one of the arms can oscillate depending on the number of modes supported by each arm. Due to short phase coherence length, the reflections do not interfere; hence the transmission through one arm is not affected due to the presence of the other. Of course this argument does not mean that Y branch operation is not valid. It is difficult to implement in practice since the electronic wavefunction does not stay coherent over the entire Y branch in the cases investigated.

One can further substantiate the validity of this model with a simple simulation shown in figure 8. Figures 8(a) and (b) show the equivalent circuit and the assumed form of the channel conductances. If the gates are driven in the same direction conductances change in the same direction and oscillations result as shown in Figure 8(c). This result is quite similar to the experimental result given in Figure 6(a). If the conductances are equal, current is divided equally; otherwise more current flows through the path with the higher conductance. On the other hand, for push pull drive one conductance monotonically increases, resulting in the monotonic increase of the current through that arm as shown in Figure 8(d). Again, this result is quite similar to the experimental results given in Figures 4, and 5. Clearly this model is valid if the transport in the output branches is diffusive rather than ballistic. If the transport is diffusive or there are no quantum effects, the conductances of output branches will change monotonically without any quantization. Figure 4(d) shows the measurement on device A at 188K. If one drives the gates in push pull, clearly a monotonic increase or decrease in the output currents results. On the other hand, oscillations are no longer observed when the gates are driven in the same direction since at this temperature transport is mainly diffusive and the quantum confinement energy is much weaker than the thermal energy. Yet there is a cross over in the currents due to the intentional offset between the output conductances as described earlier in connection with figure 7. Therefore, the observed current behavior at this temperature is due to the junction of two non-interacting classical conductances that are modified with external gate voltages.

CURRENT SWITCHING BASED ON QUANTIZED CONDUCTANCE

The mode of operation which relies on two non interacting quantized conductances still results in current switching and modulation. This mode of operation is more robust than the normal Y branch operation. First of all, it does not require wavefunction coherence over the whole device. The wavefunction only needs to be coherent over a very short length somewhere in the output branches. Furthermore, it relies entirely on quantized conductance, which is not sensitive to the energy spread of the incoming electrons provided that subband spacing is large enough. Quantized conductance can be observed even at room temperature and under realistic biases if the electron waveguide is short enough and has sufficiently strong quantum confinement. Hence a junction of two such quantized conductances can provide current switching and modulation at practical temperatures and bias conditions.

Under this mode of operation, the Y branch can function as an active device with gain. To demonstrate this potential the following experiment was performed. On device B the side gates were biased at a certain operating point and a small square wave signal was superimposed on this bias. The output currents were monitored in the configuration shown in figure 3. Depending on the bias point it is possible to get both negative and positive transconductance. In other words one of the output currents can increase and the other can decrease with increasing gate voltage as seen in Figure 6(a). The experimental results corresponding to this configuration are shown in figure 9. Indeed the output currents follow the same square wave shape, one with in phase and the other with 180° phase with respect to the gate voltage. In figure 9, only the in phase component is shown for clarity. The transconductance value depends on the slope of the output current versus gate voltage characteristics shown in figure 6(a). In the present case, transconductance is quite small since in a split gate scheme voltage applied to the gates is not very effective in modulating the channel characteristics. But in principle the output currents can be used to generate voltages by running them through resistors. If the value of this resistor is sufficiently small compared to the quantized resistance values involved, the same current switching characteristics will result. The output voltage generated this way can be applied to the gate of another structure. If the output voltage swing generated this way is larger than the input gate voltage, voltage gain can result. Therefore, such structures can drive one another and hence they may be cascaded. In the present case this would not be possible due to the inefficiency of the gate modulation on channel characteristics. But in a different geometry where this modulation is much more efficient and the quantum effects are strong, an electronic device that can drive itself may result.

CONCLUSIONS

In this paper an electron waveguide Y branch was experimentally investigated. It is found that the electronic wavefunction did not stay coherent over the entire Y branch; and hence the initially intended mode of operation is not observed. The observed current switching originates from a junction of two independent conductances. When these conductances are quantized, current switching is observed by modulating the number of modes in the output branches asynchronously. This mode of operation is different than the modal evolution in the Y branch. In this mode of operation the electron wave function needs to be coherent over a very short length somewhere in the output branches. If the

quantum confinement is strong, higher temperatures of operation under realistic bias conditions can result. Furthermore, such a switch can provide gain and could be the building block of novel quantum circuits.

ACKNOWLEDGMENTS

Authors thank Paul Maker and Richard Muller of Jet Propulsion Laboratory for the electron beam lithography. This work was supported by the NSF Science and Technology Center for Quantized Electronic Structures at UCSB (QUEST), Grant # DMR 91-20007.

REFERENCES

1. B.J. van Wees, H. van Houten, C.W.J. Beenakker, J.G. Williamson, L.P. Kouwenhoven, D. van der Marel, and C.T. Foxon, *Phys. Rev. Lett.*, **60**, 848 (1988).
2. D.A. Wharam, T.J. Thornton, R. Newbury, M. Pepper, H. Ahmed, J.E.F. Frost, D.G. Hasko, D.C. Peacock, D.A. Ritchie, and G.A.C. Jones, *J. Phys.*, **C21**, L209 (1988).
3. R. Landauer, *Philos. Mag.*, **21**, 683 (1970).
4. S. Datta, M.R. Melloch, S. Bandyopadhyay, and R. Noren, *Phys. Rev. Lett.*, **55**, 2344 (1985).
5. F. Sols, M. Macucci, U. Ravaioli, and K. Hess, *Appl. Phys. Lett.*, **54(4)**, 350, 23 Jan. 1989.
6. N. Tsukada, A. D Wieck, and K. Ploog, *Appl. Phys. Lett.*, **56(25)**, 2527, 18 June. 1990.
7. J.A. del Alamo and C.C. Eugster, *Appl. Phys. Lett.*, **56(1)**, 78, 1 Jan. 1990.
8. N. Dagli, G. Snider, J. Waldman, and E. Hu, *J. of Appl. Phys.*, **69**, 1047, (1991).
9. W. K. Burns and A. F. Milton, *IEEE J. Quantum Electronics*, **QE-11**, 32 (1975).
10. Y. Silberberg, P. Perlmutter, and J. E. Baran, *Appl. Phys. Lett.*, **51**, 1230 (1987)
11. T. Palm and L. Thylen, *Appl. Phys. Lett.*, **60**, 237 (1992)

FIGURES

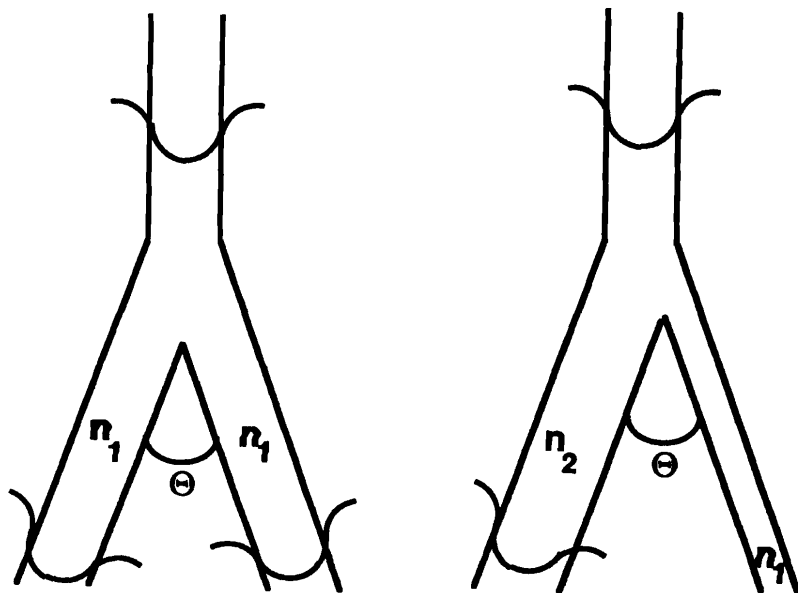


Figure 1. Schematic describing a waveguide Y branch. n_1 and n_2 refer to either the potential energy of electrons in the case of electron waves or refractive index in the case of optical waves.

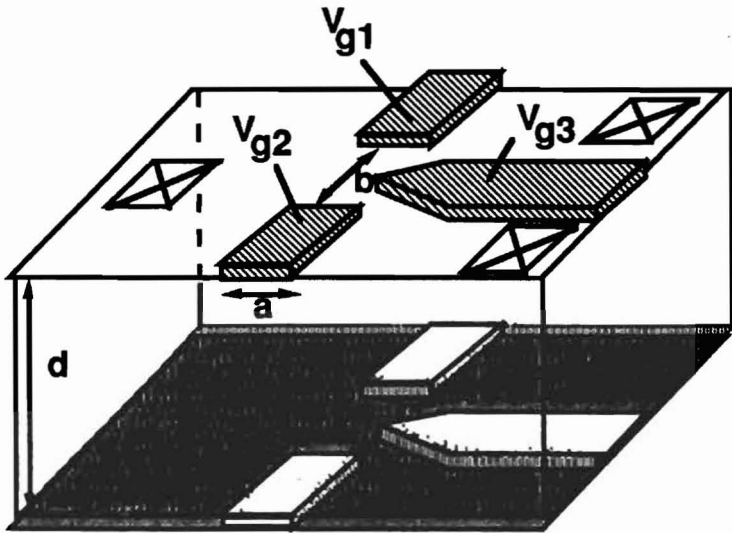


Figure 2. Plan view of electron waveguide Y branch. The upper part represents the surface. The shaded rectangles and crossed rectangles on the surface indicate Schottky gates and ohmic contacts, respectively. The gray area below represents electrons in the plane of the 2DEG. Electrons are depleted immediately underneath the gates with applied voltages V_{g1} , V_{g2} , and V_{g3} , forming a Y branch.

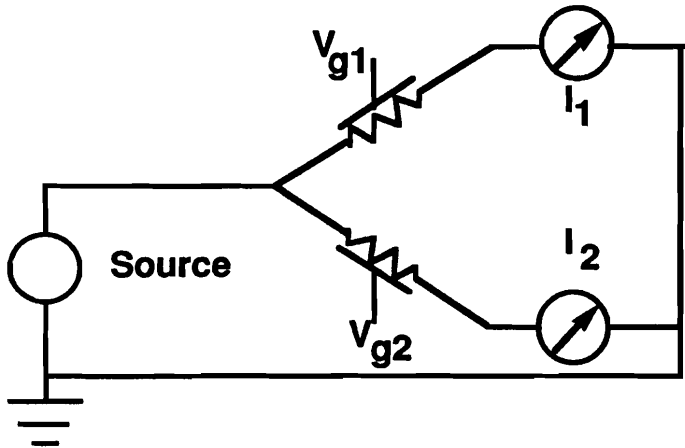
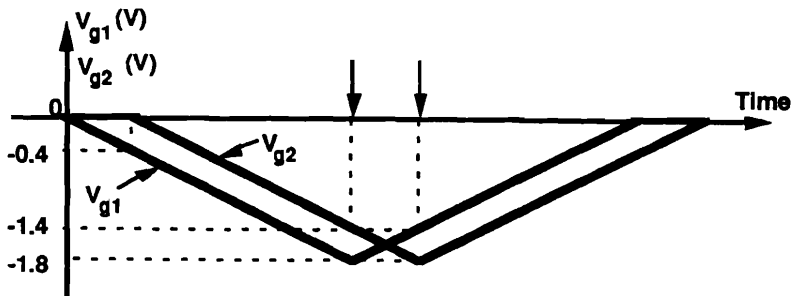
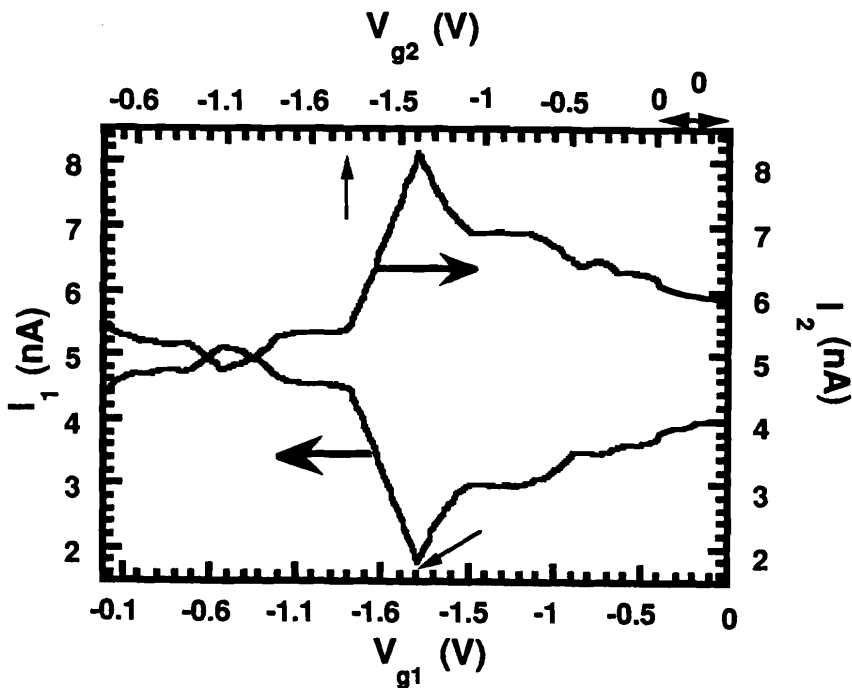


Figure 3. Schematic describing the measurement conditions on the Y branch. A constant voltage or constant current source drives the input of the Y. The current flowing through each arm is measured as a function of gate voltages V_{g1} and V_{g2} . V_{g3} was kept constant during the measurements.



(a)



(b)

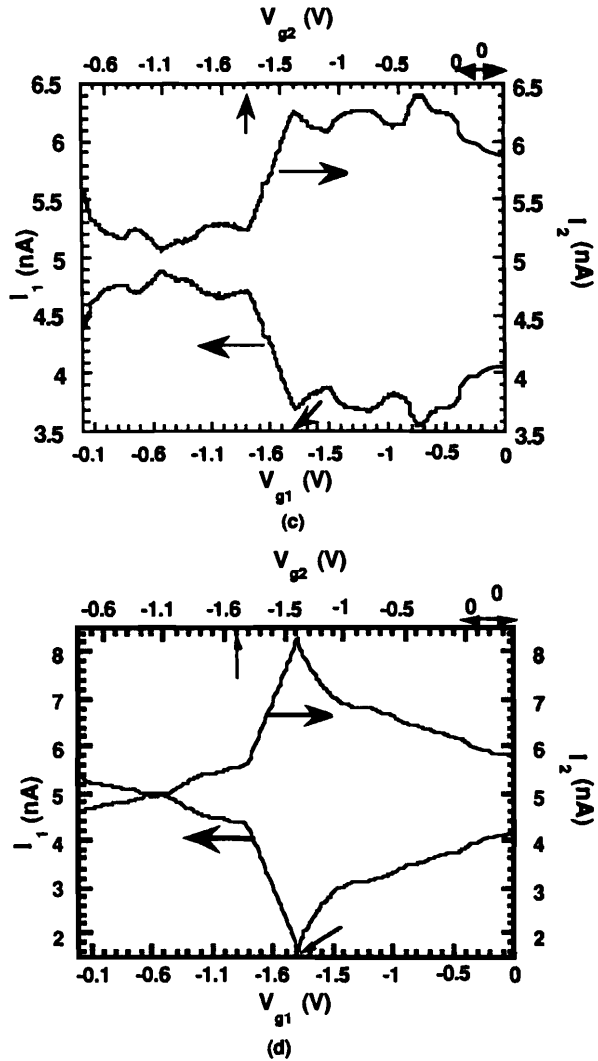


Figure 4. Currents in the output branches of device A as a function of the gate voltages V_{g1} and V_{g2} when a constant current source of 10 nA drives the input. V_{g3} was kept constant at -900 mV. (a) The timing of the V_{g1} and V_{g2} with respect to each other, (b) The results at 4.2 Kelvin, (c) The results at 0.3 Kelvin, (d) The results at 188 Kelvin.

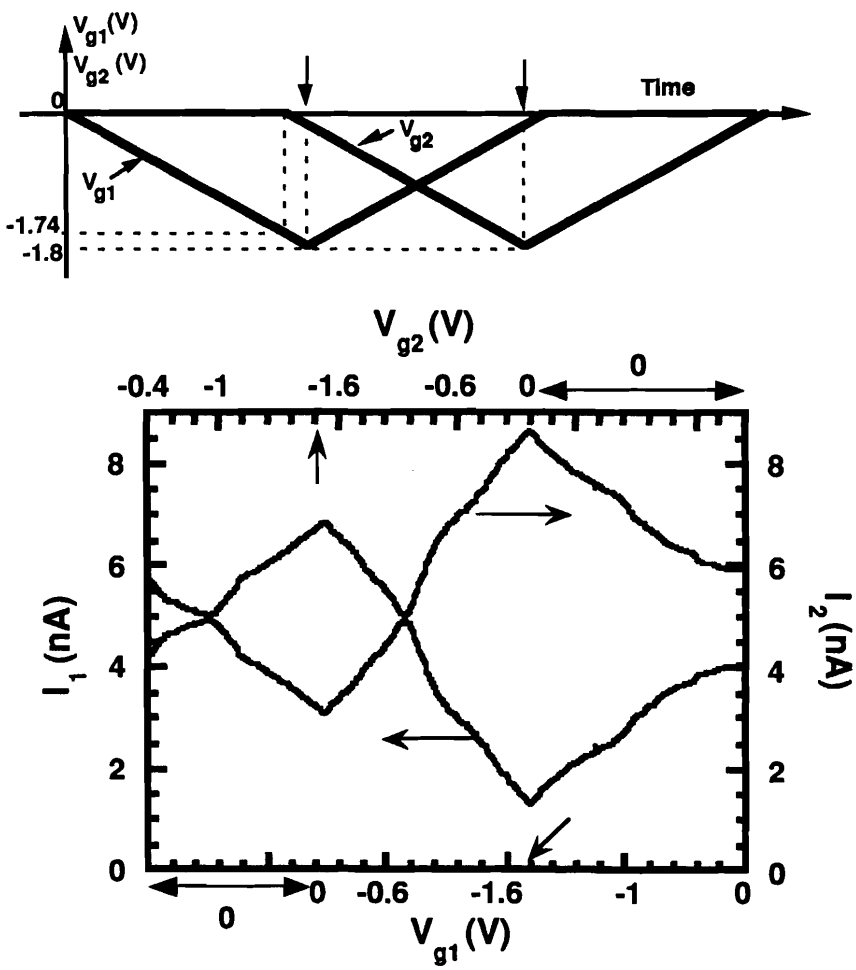
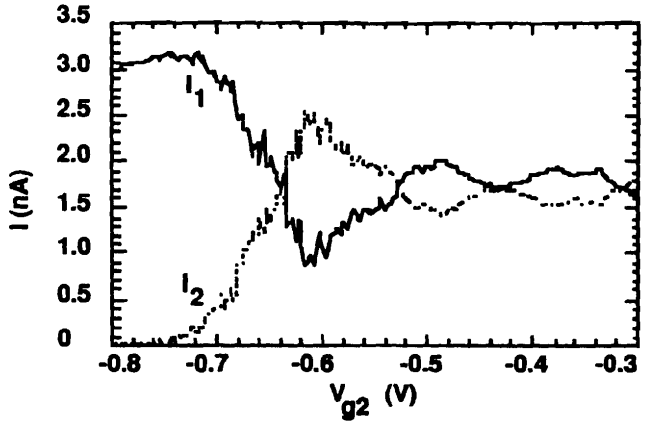
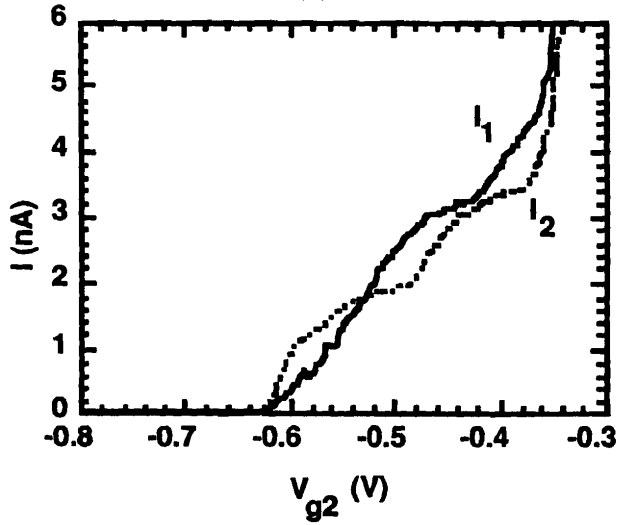


Figure 5. Currents in the output branches of device A as a function of the gate voltages V_{g1} and V_{g2} when a constant current source of 10 nA drives the input. V_{g3} was kept constant at -900 mV. The timing of the V_{g1} and V_{g2} with respect to each other are shown in the upper part of the figure. The data was taken at 4.2 Kelvin.



(a)



(b)

Figure 6. Currents in the output branches of device B as a function of gate voltage $V_{g2} = V_{g1}$. V_{g3} is kept constant at -800mV . The data was taken at 4.2 Kelvin , (a) when a constant current source of 3nA drives the input, (b) when a constant voltage source of $26\mu\text{V}$ drives the input.

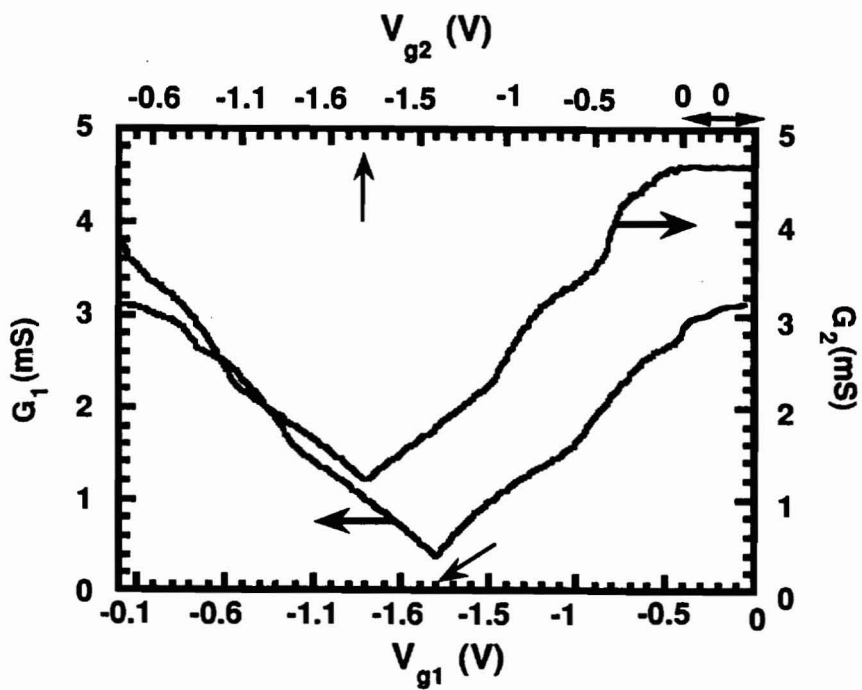


Figure 7. Conductances of the output branches of device A corresponding to the measurement shown in Figure 4(b).

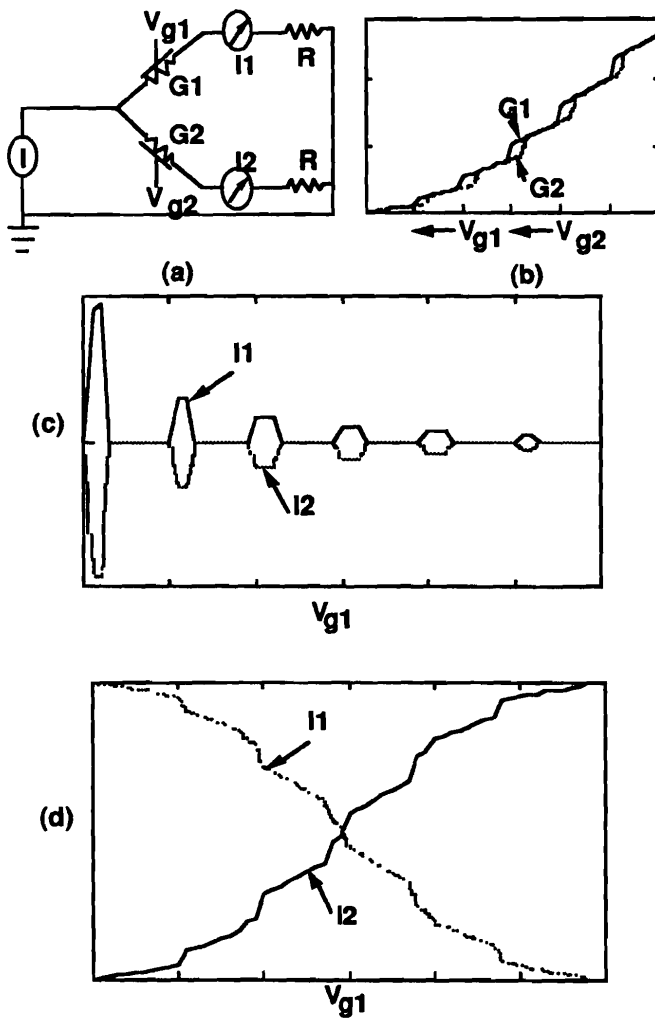


Figure 8. (a) Equivalent circuit of the Y branch when output branches are modeled as independent conductances. (b) Assumed form of the output conductances $G1$ and $G2$ as a function of the gate voltages defining the output channels. A slight asymmetry is assumed between $G1$ and $G2$. (c) Resulting output currents when side gate voltages are driven in the same direction and $V_{g1} = V_{g2}$. (d) Resulting output currents when side gate voltages are driven in opposite directions.

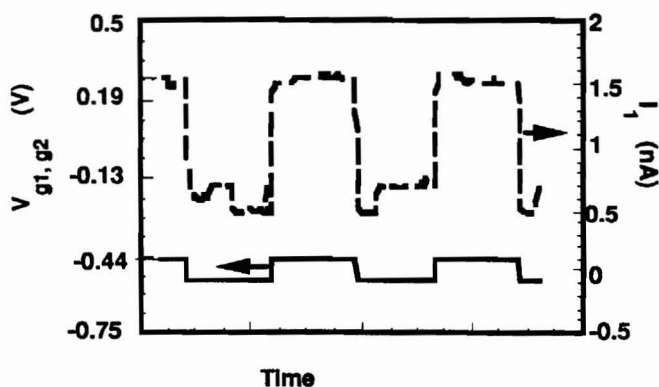


Figure 9. One of the output currents, I_1 , of device B as a function of the voltage applied to the side gates, $V_{g1} = V_{g2}$. V_{g3} is kept constant at -800 mV. The other output current, I_2 , is $I_2 = 3$ nA $- I_1$. This component is not shown in the figure for clarity. The actual values on the time axis are not shown but the frequency of the square wave modulation is 1 MHz. The data was taken at 4.2 Kelvin.